Towards Release-Free Intermodal Acousto-Optic Modulation at Visible and UV Wavelengths

CNF Project Number: 2985-21

Principal Investigator(s): Karan Kartik Mehta (2)

User(s): Oscar Jaramillo(1, 2)

Affiliation(s): School of Applied and Engineering Physics, Cornell University (2) School of Electrical and Computer Engineering, Cornell University

Primary Source(s) of Research Funding: NSF

Contact: karanmehta@cornell.edu, oj43@cornell.edu

Primary CNF Tools Used: Zeiss Ultra SEM, PT770 Etcher, Woollam RC2 Spectroscopic Ellipsometer, SC4500 Evaporator, Oxford PECVD, Keyence VHX-7100 Digital Microscope, Oxford FlexAL, OEM Endeavor M1, ASML Stepper

Abstract:

We present an inter-modal acousto-optic modulator designed to operate near $\lambda \sim 405$ nm, leveraging acoustic modes confined and co-localized with a buried optical waveguide. We demonstrate the acoustic waveguiding concept, predicted to enable opto-mechanical coupling coefficient $g \approx 2$ (sqrt(μ W)mm)⁻¹.

Summary of Research, 2023-2024 Progress:

Acousto-optic modulators (AOMs) are widely used for frequency, phase, and amplitude control in a broad range of applications. Tabletop systems suffer from a relatively large footprint since the acoustic power is delocalized relative to the optical power. As a result, they typically consume on the order of 1-10 Watts, limiting their scalability and compatibility with multiplexed on-chip systems. Promising efficiencies of on-chip AOMs

have been demonstrated at $\lambda \sim 780\text{-}1550$ nm^[1-4]. In certain cases, the use of non-standard CMOS materials and/or the fabrication complexity—such as released structures—pose challenges for large-scale integration. Furthermore, the materials employed to date are lossy in the UV and visible, essential for a variety of applications such as bio-chemical spectroscopy, and quantum control of trapped ions, neutral atoms, and solid-state quantum systems ^[5,6].

We present a design for robust, low-power, compact, and CMOS-compatible on-chip AOMs in the blue and UV, and demonstrate the fundamental waveguiding principle in our concept, towards scalable modulation for atomic systems. The concept leverages the high refractive index (RI) contrast offered by HfO2-Al2O3 composites $^{[7]}$, resulting in high opto-mechanical coupling coefficient g owing to 3 scaling from photoelasticity and $\sim \epsilon^2 (\epsilon \text{clad}^{-1} - \epsilon \text{core}^{-1})$ core from waveguide boundary movement $^{[1]}$.

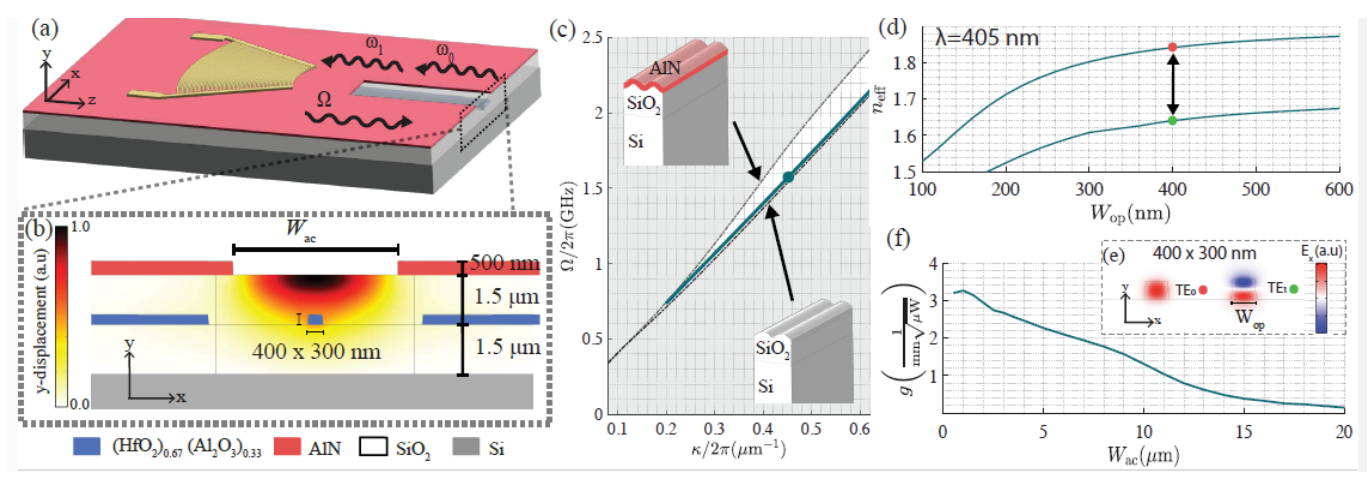


Figure 1: a) Schematic of a release-free AOM with co-confined acoustic and optical modes. (b) Cross section showing the dominant (y) displacement of a confined acoustic mode. c) Dispersion of guided mode with top (bottom) light-cone of a AlN+SiO₂ (SiO₂) RM. d) Effective index $n_{\rm eff}$ of optical modes vs optical waveguide width $W_{\rm op}$ with points representing modes used to calculate g. Gray modes are the non phase-matched modes. f) Simulated g for a 400 ×300 nm optical waveguide vs acoustic waveguide width ($W_{\rm ae}$). Use of buried optical waveguides facilitates integration in CMOS- like stacks, along with integration of additional photonic waveguide layers for mode demultiplexing.

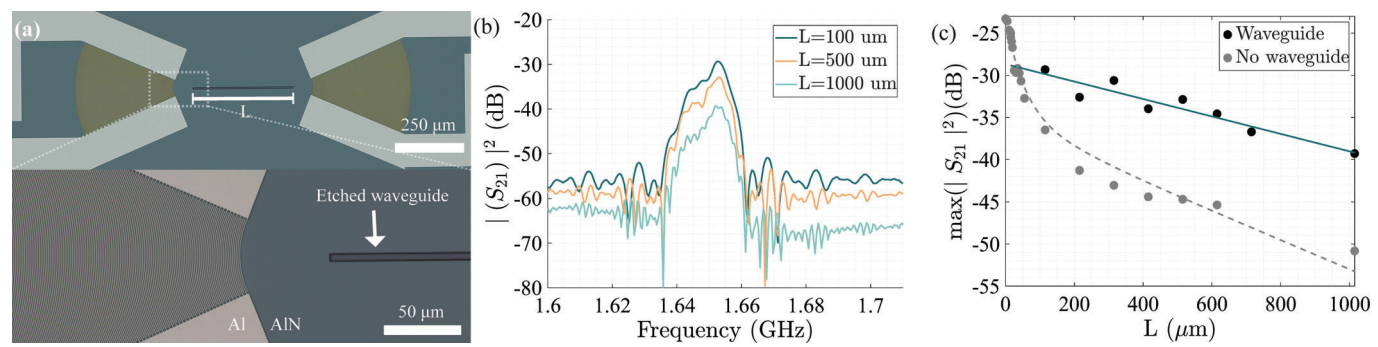


Figure 2: . a) Micrograph of a fabricated device with acoustic waveguide length L. b) Subset of representative |S12|2 curves. c) Peak values for |S12|2 vs L for structures without and with the acoustic waveguide etched, indicating clear acoustic guiding.

Our AOM is composed of a (HfO₂)₆₇(Al2O₃)₆₇ multimode optical-waveguide buried in SiO2 and a 500 nm thick film of sputtered AlN used to launch a counterpropagating acoustic wave via a focusing inter-digitated transducer (Fig. 1a). The overall film stackup supports a RM (top inset of Fig. 1c), which together with an etched trench of width W_{ac} on AlN, creates a confined acoustic mode that overlaps with the buried optical waveguide (Fig. 1b). This mode is characterized by its dominant displacement along the y- direction, which shifts the top and bottom boundaries of the optical mode, coupling the TE₀ and the TE₁ modes at $\lambda = 405$ nm (Fig. 1d). As W decreases, the acoustic energy overlap with the waveguide increases, resulting in a higher g. The acoustic wave induces oscillations in power between the optical modes, achieving full conversion from the TE₀ to the TE₁ mode at an acoustic power of $P_{\pi/2} = (\pi/(2gL_{\text{eff}}))^2$, where $L_{\rm eff} = (1 - \exp(-\alpha_{\rm wg} L))/\alpha_{\rm wg}$ is the effective length and $\alpha_{\rm wg}$ is the acoustic waveguide loss.

To demonstrate the acoustic guiding principle, we design and fabricate the device from Fig. 1a without the optical waveguide. We sputter ~500 nm of AlN on 3 um of thermal SiO2, pattern the electrodes with 100 nm of aluminum using a lift-off process and etch the waveguide with a dry etch process. A fabricated device with acoustic waveguide length L= 500 μm is shown in Fig. 2a. To estimate propagation loss ignoring reflections, we measure S21 for L varying from 100 to 1000 µm (Fig. 2b) and take the peak value as the transmission (Fig. 2c). A fit to $max(|S_{12}|^2) = \eta^2 exp(-1)$ $\alpha_{_{\!\scriptscriptstyle \mathsf{U\!\!\!\!U}\!\!\scriptscriptstyle o}} L)$ indicates a transducer-WG coupling efficiency $|\eta| = -14.4 \pm 0.4 \text{ dB}$ and $\alpha_{wg} = 10.3 \pm 1.6 \text{ dB/mm}$. Fig 2c also shows measurements of the same device prior to trench etching, demonstrating that as L increases, the transmission follows our model, which accounts for losses due to mode mismatch from defocusing, along with a Rayleigh-mode (RM) loss of approximately αRM ~9 dB/mm. With the etched waveguide, the transmission remains linear for an etched waveguide, indicating the functioning of the acoustic guiding. The measured

transduction efficiency and acoustic waveguide loss project that a device with the $(HfO_2)_{.67}(Al_2O_3)_{.33}$ film should exhibit full mode-conversion in L= 100 μ m with an RF driving power below 2.5 mW.

This work establishes an efficient platform for onchip inter-modal acousto-optic modulation in a CMOS compatible and release-free configuration at blue and UV wavelengths. Realization of the full acousto-optic device leveraging the demonstrated optical and acoustic waveguides and transducers together is in progress. This platform may enable foundry-compatible efficient active control of UV and visible light in integrated systems.

References:

- [1] C. J. Sarabalis et al., "Acousto-optic modulation of a wavelength-scale waveguide," Optica 8, 477–483 (2021).
- [2] L. Zhang et al., "Integrated-waveguide-based acousto-optic modulation with complete optical conversion," Optica 11, 184–189 (2024).
- [3] E. A. Kittlaus et al., "Electrically driven acousto-optics and broadband non-reciprocity in silicon photonics," Nat. Photonics 15, 43–52 (2021).
- [4] Q. Lin et al., "Optical multi-beam steering and communication using integrated acousto-optics arrays," Nat. Commun. 16, 1–7 (2025).
- [5] D. J. Blumenthal, "Photonic integration for UV to IR applications," APL Photonics 5 (2020).
- [6] G. Moody et al., "2022 roadmap on integrated quantum photonics," J. Phys.: Photonics 4, 012501 (2022).
- [7] O. Jaramillo et al., "HfO₂-based platform for high-indexcontrast visible and UV integrated photonics," Opt. Lett. 50, 3165–3168 (2025).